Stem Cell Reports, Volume *18*

Supplemental Information

Segregation of the stemness program from the proliferation program in intestinal stem cells

Yuan Liu, Meimei Huang, Xiaodan Wang, Zinan Liu, Siqi Li, and Ye-Guang Chen

Fig S1

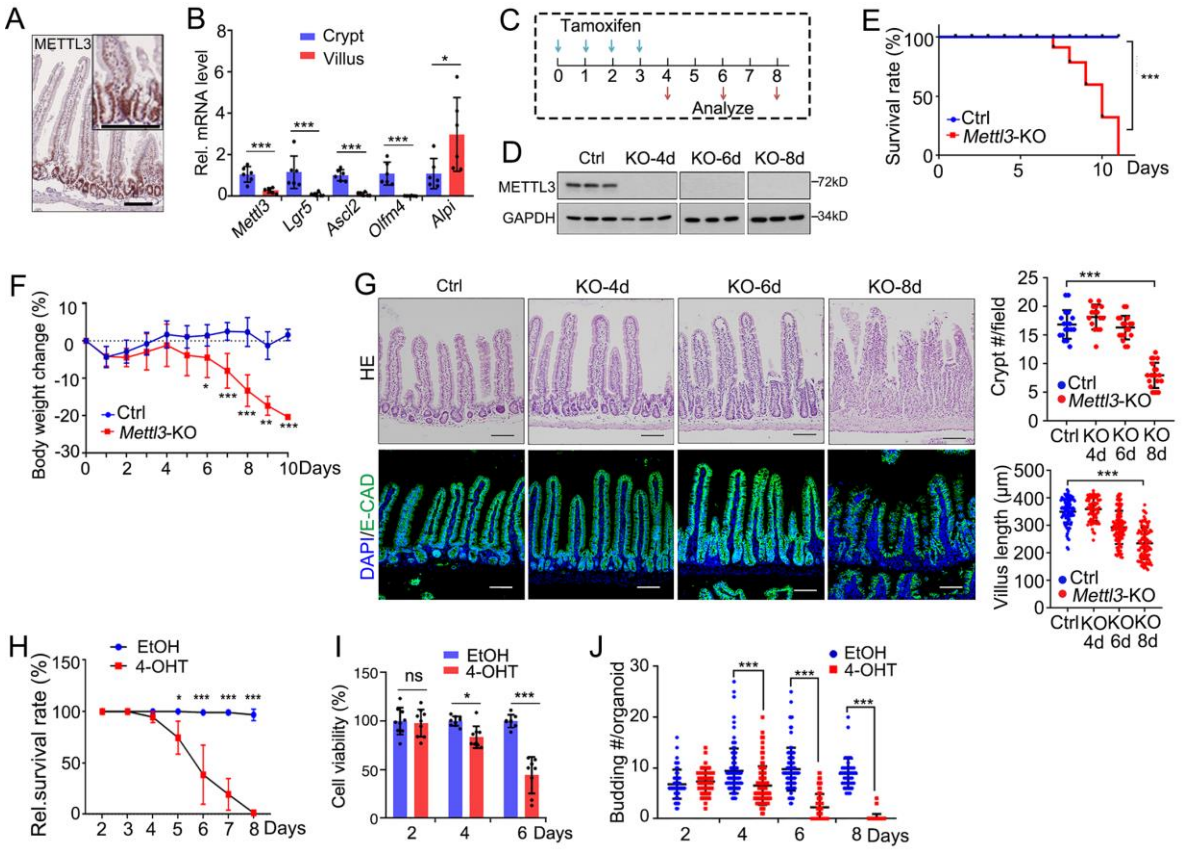

Figure S1. *Mettl3* is required for small intestine maintenance, related to Figure 1.

(A) Immunohistochemical staining of METTL3 in the jejunum. (B) q-PCR analysis of *Mettl3*, *Lgr5*, *Ascl2*, *Olfm4* and *Alpi* gene expression in jejunum crypt and villus. N=6 mice. (C) Schematic of tamoxifen treatment regimen and analysis of tissues from control (*Mettl3*$^{fl/fl}$) and *Mettl3*-KO (*Villin-CreERT2;Mettl3*$^{fl/fl}$) mice after tamoxifen (TAM) injection at the indicated time. (D) Immunoblot of METTL3 protein expression in intestinal crypt epithelium isolated from control (*Mettl3*$^{fl/fl}$) and *Mettl3*-KO mice (*Villin-CreERT2;Mettl3*$^{fl/fl}$) at indicated time after TAM injection. GAPDH, loading control. N=3 mice/group. (E) Survival plot for control (*Mettl3*$^{fl/fl}$) and *Mettl3*-KO (*Villin-CreERT2;Mettl3*$^{fl/fl}$) mice of 8-10 weeks old after injected with 20 mg/mL TAM for 4 days. N=11 mice/group. (F) Body weight following TAM injection of control (*Mettl3*$^{fl/fl}$) and *Mettl3*-KO (*Villin-CreERT2;Mettl3*$^{fl/fl}$) mice. N=9 mice/group. (G) Representative hematoxylin and eosin (HE) and immunofluorescence staining of the jejunum from control (*Mettl3*$^{fl/fl}$) and *Mettl3*-KO (*Villin-CreERT2;Mettl3*$^{fl/fl}$) mice at the indicated time after first TAM injection. Crypt number and villus length were shown in the right. N=3 mice/group, n=5 fields/mouse, n>100 villi/group. (H-J) Survival rate (H), cell viability (I) and budding number (J) in the organoids derived from *Mettl3*$^{fl/fl}$*;Villin-CreERT2* mice at the indicated time following EtOH or 4-hydroxytamoxifen (4-OHT) treatment for 2 days. N>100 organoids/group from three independent experiments. Nuclei were counter-stained with DAPI. The data represent mean±SD. *** P<0.001, ** P<0.01, * P<0.05, one-way ANOVA (G), two-way ANOVA (B, F, H, I and J), Log-rank test (E). Scale bars: 100 μm (A and G).

Fig S2

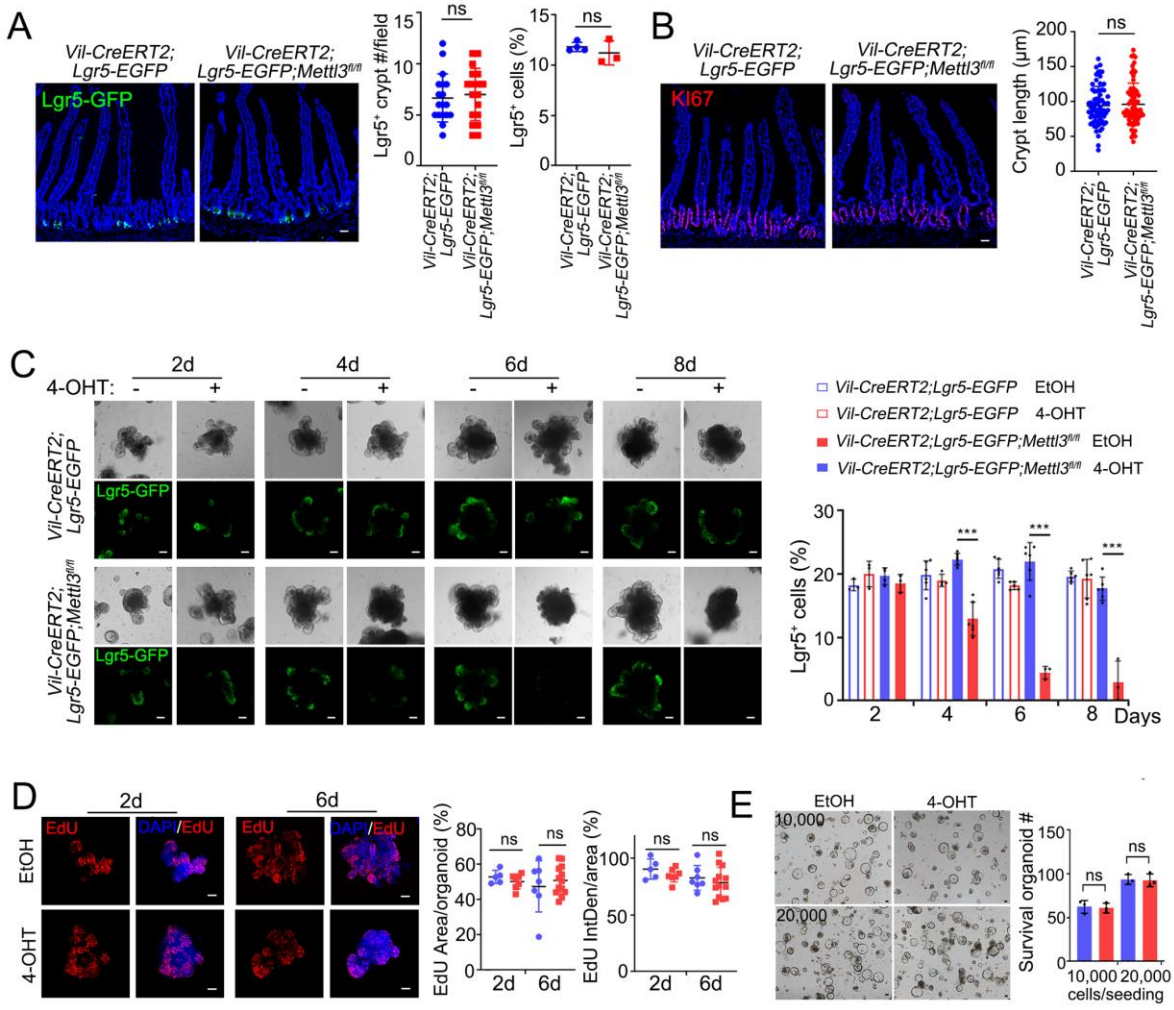

Figure S2. *Mettl3* is required for the development and maintenance of small intestine, related to Figure 1 and 2.

(A, B) Representative images and quantification of Lgr5-GFP$^+$ cells and KI67$^+$ cells in the jejunum of mice at 6 dpt. *Vil-CreERT2;Lgr5-EGFP* and *Vil-CreERT2;Lgr5-EGFP;Mettl3$^{fl/fl}$* mice were treated with TAM and oil, respectively. N=3 mice/group. (C) Representative images and quantification of Lgr5-GFP$^+$ cells in organoid derived from *Vil-CreERT2;Lgr5-EGFP* and *Vil-CreERT2;Lgr5-EGFP;Mettl3$^{fl/fl}$* mice after EtOH or 4-OHT treatment. Data from three independent experiments were combined and shown. (D) Representative images and quantification of EdU$^+$ cells in organoid derived from *Vil-CreERT2;Lgr5-EGFP* mice at 2 or 6 dpt. N=5-13 organoids/group from three independent experiments. (E) Representative images (left) and quantification (right) of intestinal organoids cultured from sorted Lgr5-GFP$^+$ cells derived from *Lgr5-EGFP-IRES-CreERT2;Mettl3$^{w/w}$* mice after treated with EtOH or 4-OHT for 5 days. The number of seeded cells was 10,000 and 20,000. Data from three independent experiments were combined and shown. Nuclei were counter-stained with DAPI. The data represent mean±SD. *** P<0.001, ** P<0.01, * P<0.05, unpaired two-tailed t-test (A, B), two-way ANOVA (C, D and E). Scale bars: 50 μm (A-E).

Fig S3

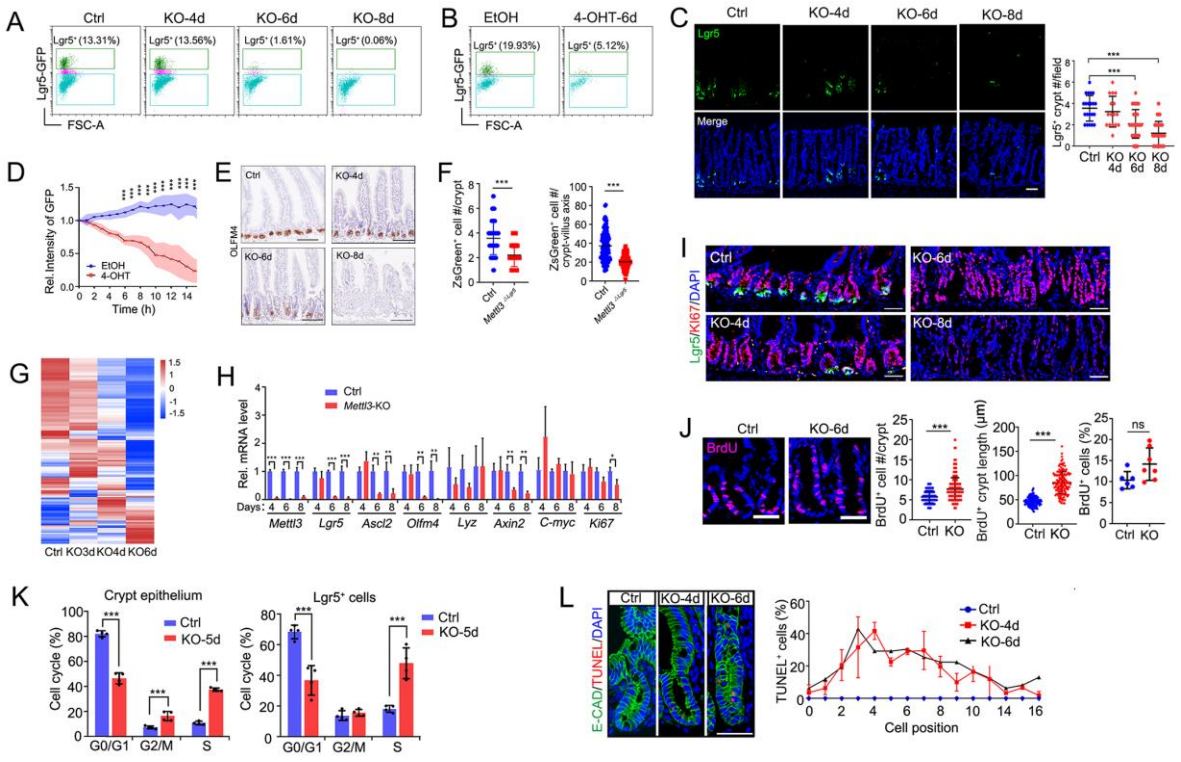

Figure S3. *Mettl3* deletion leads to loss of intestinal stem cells, hyper-proliferation and cell death in crypts, related to Figure 1.

(A) Lgr5-GFP^{+} cells in the crypts from control and *Mettl3*-KO-GFP mice at the indicated time, as revealed by FACS. (B) Lgr5-GFP^{+} cells of the organoids derived from *Vil-CreERT2;Lgr5-EGFP-IRES-CreERT2;Mettl3$^{fl/fl}$* mice at day 6 after treated with EtOH or 4-OHT for 2 days. (C) Representative images and quantification of Lgr5-GFP^{+} stem cells in the colon of control and *Mettl3*-KO-GFP mice at the indicated time after TAM injection. N=3 mice/group, n=5-10 fields/mouse. (D) Quantification of relative average fluorescence intensity of Lgr5-GFP at 1h intervals at day 4.5 after EtOH or 4-OHT treatment for 2 days, as revealed by confocal microscopy. N=5 organoids/group from three independent experiments. (E) Immunohistochemical staining of OLFM4 in the jejunum of control (*Mettl3$^{fl/fl}$*) and *Mettl3*-KO (*Vil-CreERT2;Mettl3$^{fl/fl}$*) mice at indicated times after TAM injection. (F) Quantification of ZsGreen^{+} cell number in the jejunum of control *(Lgr5-CreERT2;Rosa26$^{loxp\text{-}stop\text{-}loxp\text{-}ZsGreen}$*) and *Mettl3$^{\Delta Lgr5}$* (*Mettl3$^{fl/fl}$;Lgr5-CreERT2;Rosa26$^{loxp\text{-}stop\text{-}loxp\text{-}ZsGreen}$*)mice at 1dpt (left) and 4dpt (right) hours. N=4 mice/group, n>100 crypts/group. (G) Heatmap showing the differential expression of the 384 stem cell signature genes in Lgr5-GFP^{+} ISCs from control and *Mettl3*-KO-GFP mice. (H) q-PCR shows the expression of *Mettl3*, *Lgr5*, *Ascl2*, *Olfm4*, *Lyz*, *Axin2*, *C-myc* and *Ki67* in jejunum crypts of control (*Mettl3$^{fl/fl}$*) and *Mettl3*-KO (*Vil-CreERT2;Mettl3$^{fl/fl}$*) mice after injection with Tamoxifen at indicated time. N=3 mice/group. (I) Immunofluorescence co-staining of Lgr5-GFP and KI67 in the jejunum of control and *Mettl3*-KO-GFP mice at the indicated time after TAM injection. (J) A jejunum section showing BrdU^{+} cells at 2 hours after one dose injection of BrdU in control (*Mettl3$^{fl/fl}$*) and *Mettl3*-KO (*Vil-CreERT2;Mettl3$^{fl/fl}$*) mice at 6 dpt. Quantification of BrdU-labeled cell number and crypt length at 2 hours after BrdU injection. N=3 mice/group, n>100 crypts/group. (K) Cell cycle stage distribution of the crypt epithelial cells (left) and Lgr5-GFP^{+} cells (right) in control and *Mettl3*-KO-GFP

mice at 5 dpt. N=4 mice/group. (L) Representative images (left) and quantification (right) of TUNEL$^+$ cell position in jejunum crypts of control (*Mettl3*$^{fl/fl}$) and *Mettl3*-KO (*Vil-CreERT2;Mettl3*$^{fl/fl}$) mice at the indicated time after TAM injection. The cell boundary was defined by E-cadherin. N=4 mice/group. The littermate mice (*Villin-CreERT2;Lgr5-EGFP-IRES-CreERT2;Mettl3*$^{fl/fl}$) were treated with TAM (*Mettl3*-KO-GFP) or Oil (control) (A, C, G, I, K). All the data represent mean±SD. *** P<0.001, ** P<0.01, * P<0.05, one-way ANOVA (C), two-way ANOVA (D, H, K and L), unpaired two-tailed t-test (F and J). Scale bars: 50μm (C, I, J and L), 100μm (E). Nuclei were counter-stained with DAPI.

Fig S4

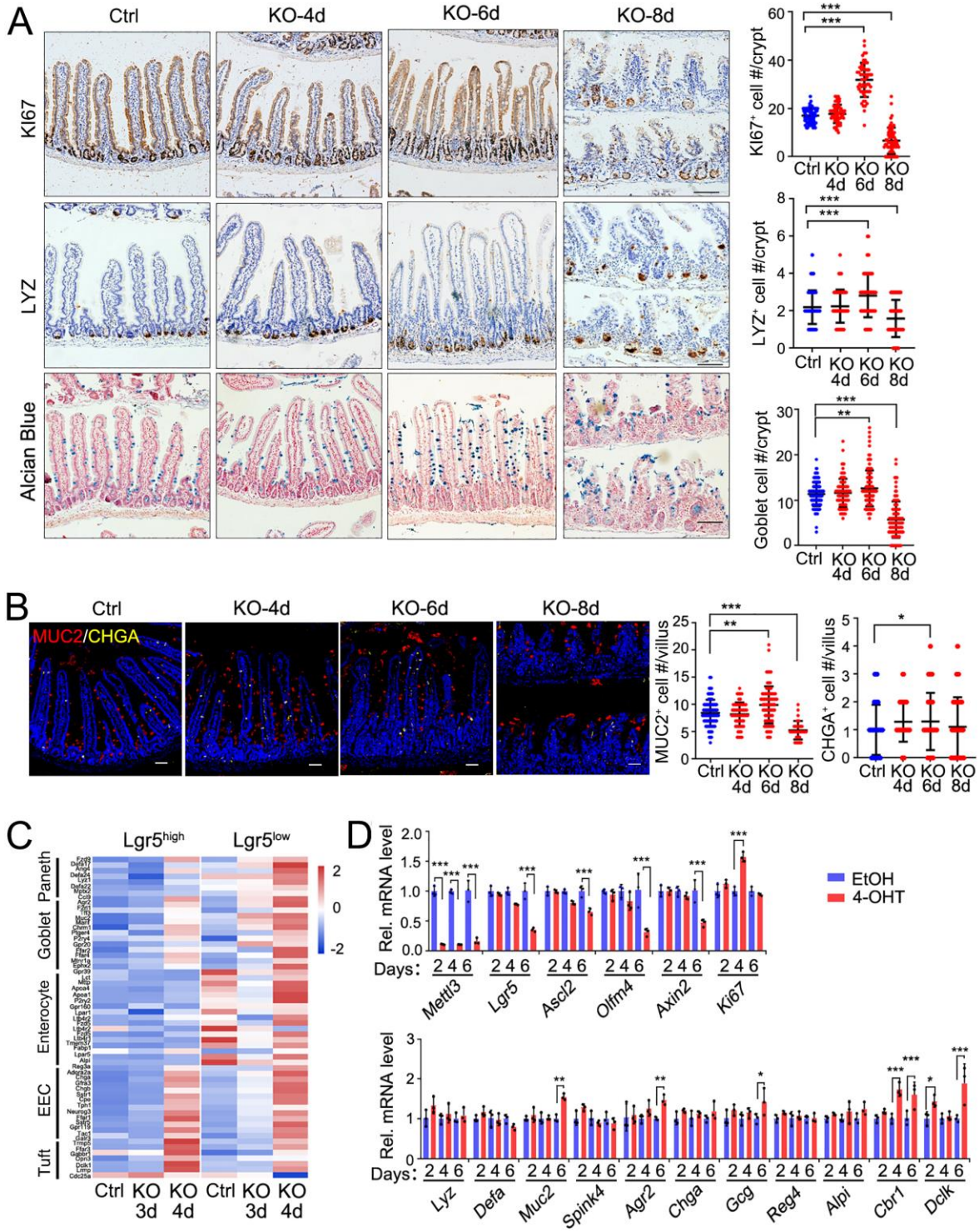

Figure S4. Mild effect on cell differentiation in *Mettl3*-KO mice, related to Figure 1.

(A) Immunohistochemical staining and quantification of KI67$^+$ cells, LYZ$^+$ cells and goblet cell (Alcian blue staining) in the jejunum of control (*Mettl3*$^{fl/fl}$) and *Mettl3*-KO (*Villin-CreERT2;Mettl3*$^{fl/fl}$) mice after injection with TAM at the indicated time. N=3 mice/group, n=5 fields/mouse, n>100 crypts or villi per group. (B) Immunofluorescence co-staining of MUC2 and CHGA and quantification (right) in the jejunum of control (*Mettl3*$^{fl/fl}$) and *Mettl3*-KO (*Villin-CreERT2;Mettl3*$^{fl/fl}$) mice after injection with TAM at

the indicated time. Nuclei were counter-stained with DAPI. N=3 mice/group, n=5 fields/mice, n>100 crypts or villi per group. (C) Expression heatmap of differentiated cell signature genes in Lgr5^{high} and Lgr5^{low} cells from control and *Mettl3*-KO-GFP mice at the indicated time. The littermate mice (*Villin-CreERT2;Lgr5-EGFP-IRES-CreERT2;Mettl3$^{fl/fl}$*) were treated with TAM (*Mettl3*-KO-GFP) or Oil (control). (D) qPCR shows gene expression in the organoids derived from *Villin-CreERT2;Mettl3$^{fl/fl}$* mice at indicated time after treated with EtOH or 4-OHT for 2 days. Data from three independent experiments were combined and shown. All the data represent mean ±SD. *** P<0.001, ** P<0.01, * P<0.05, one-way ANOVA (A, B), two-way ANOVA (D). Scale bars: 100 μm (A), 50 μm (B).

Fig S5

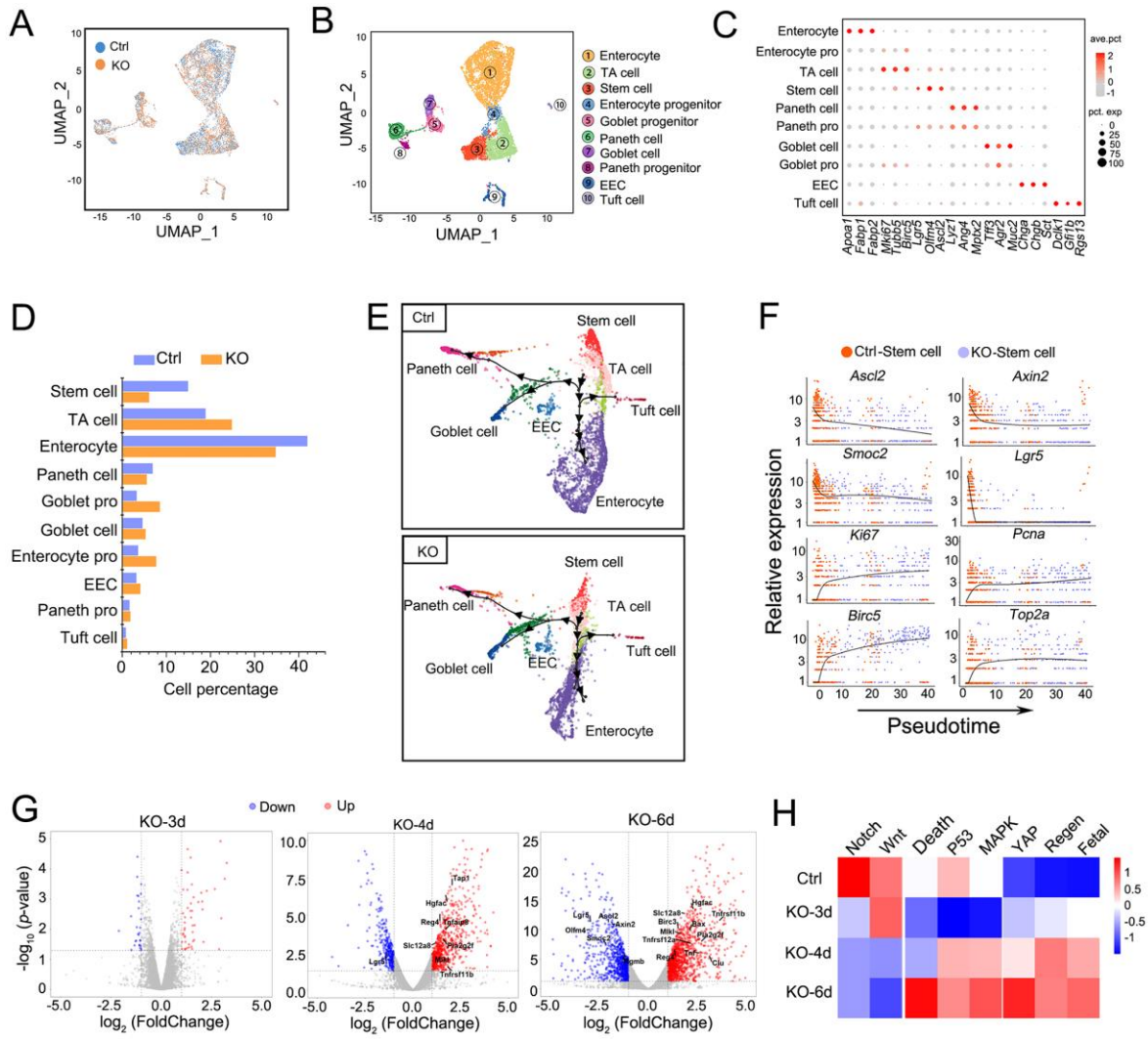

Figure S5. sc-RNA-seq analysis reveals impaired intestinal stem cells and the high proliferation property in stem cells in *Mettl3*-KO-GFP mice, related to Figure 3 and 4.

(A and B) scRNA-seq analysis of small intestinal epithelium from control and *Mettl3*-KO-GFP mice as visualized by UMAP. (C) Dot plot showing scaled expression level (color scale) and percent of expressing cells (point diameter) of the marker genes in each cell cluster. (D) The cell ratio of each cell type in the small intestinal epithelium of control and *Mettl3*-KO-GFP mice at 4 dpt. (E) Pseudotime analysis of all cell types in control and *Mettl3*-KO-GFP mice, based on scRNA-seq. The arrangement of cell clusters in *Mettl3*-KO-GFP mice on the pseudotime line was based on the cells in control mice. The points were lined according to the cell fate stage with stem cell cluster as the starting point. (F) The expression of the stem cell markers (*Ascl2*, *Axin2*, *Smoc2* and *Lgr5*) and the TA cell markers (*Ki67*, *Pcna*, *Birc5* and *Top2a*) in control stem cells and KO stem cells, plotted along the above-defined pseudotime axis in Fig. 3F. (G) Volcano plots depict differentially expressed genes in Lgr5$^+$ cells upon *Mettl3* KO for the indicated time in comparison with control mice. Red and blue dots correspond to the upregulated genes ($log_2FC \geq 1$, $p<0.05$) and downregulated genes ($log_2FC \leq -1$, $p<0.05$), respectively. (H) GSEA analysis of signaling pathways in Lgr5$^+$ ISCs upon *Mettl3* KO. NES was considered as the original values to draw the heatmap. The littermate mice (*Villin-CreERT2;Lgr5-*

EGFP-IRES-CreERT2;Mettl3$^{fl/fl}$) were treated with TAM (*Mettl3*-KO-GFP) or Oil (control).

Fig S6

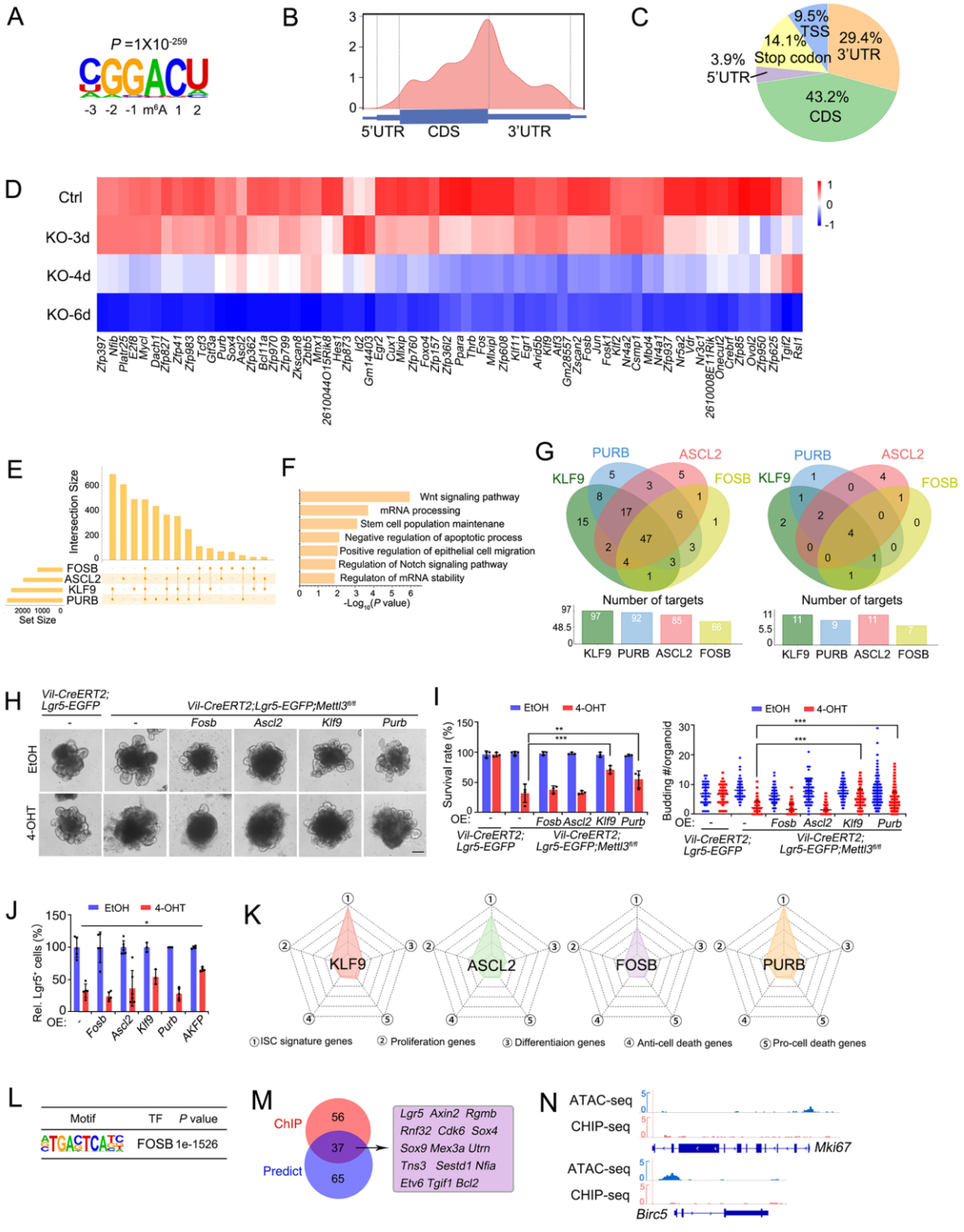

Figure S6. ASCL2, KLF9, FOSB and PURB restore the stem gene expression in the *Mettl3*-KO-GFP organoids, related to Figure 5 and 6.

(A) Consensus m6A modification sequence identified within m6A peaks by HOMER. (B and C) Metagene profiles (B) and pie chart (C) of m6A peak distribution along a normalized transcript composed of three rescaled non-overlapping segments: 5′UTR, CDS, and 3′UTR. (D) Expression

heatmap of transcription factors whose m6A modification was reduced upon *Mettl3* knockout. (E) UpsetR visualizes the overlap of the predicted target genes of AKFP. (F) GO analysis of all predicted target genes of AKFP. (G) Venn diagram indicates predicted target gene number regulated by AKFP of the down-regulated genes from 384 stem cell signature gene (left) and the 23 filter stemness gene (right). (H and I) Representative image (H), quantification of survival rate (I, left) and budding number (I, right) of the organoids expressing *Fosb*, *Ascl2*, *Klf9* or *Purb*. The organoids were derived from *Villin-CreERT2;Lgr5-EGFP-IRES-CreERT2;Mettl3*$^{fl/fl}$ or *Villin-CreERT2;Lgr5-EGFP-IRES-CreERT2* mice at day 5 after EtOH or 4-OHT treatment for 2 days. Scale bars: 100 μm. N>100 organoids/group from three independent experiments. (J) Relative Lgr5-GFP^{+} cell number in of the organoids expressing *Fosb*, *Ascl2*, *Klf9*, *Purb* or all of them (*AKFP*). The organoids were derived from *Mettl3*$^{fl/fl}$*;Villin-CreERT2;Lgr5-EGFP-IRES-CreERT2* or *Villin-CreERT2;Lgr5-EGFP-IRES-CreERT2* mice at day 6 after EtOH or 4-OHT treatment for 2 days. Data from three independent experiments were combined and shown. (K) Function characteristics distribution of the predicted target genes of KLF9, ASCL2, FOSB and PURB, respectively. (L) HOMER motif of FOSB ChIP-seq. (M) Venn diagram displays the overlap genes between predicated stem cell signature targets of Fosb (blue) and the genes confirmed by anti-FOSB ChIP-seq (red). (N) FOSB ChIP-seq and ATAC-seq tracks of the proliferation genes *Ki67* and *Birc5*. The littermate mice (*Villin-CreERT2;Lgr5-EGFP-IRES-CreERT2;Mettl3*$^{fl/fl}$) were treated with TAM (*Mettl3*-KO-GFP) or Oil (control) (A-D). All data represent mean±SD. *** P<0.001, ** P<0.01, two-way ANOVA (I and J).

Movie S1: **Time-lapse Video shows representative buds of organoids expressing Lgr5-EGFP (green) following 4-OHT treatment.** Organoids derived from *Villin-CreERT2;Lgr5-EGFP-IRES-CreERT2;Mettl3*$^{fl/fl}$ mice were imaged every 1h from day 4.5 to day 6.5 after treated with EtOH (left) or 4-OHT and labeled with CellMask (Orange plasma membrane stain, red). Video shows the change of Lgr5-GFP cells over time from 0 h to 20 h.

Table S1: Mouse model.

Label	Genotyping	Treatment
Control	*Mettl3*$^{fl/fl}$	TAM
Mettl3-KO	*Villin-CreERT2;Mettl3*$^{fl/fl}$	TAM
Control	*Lgr5-EGFP-IRES-CreERT2;Villin-CreERT2;Mettl3*$^{fl/fl}$	Oil
Mettl3-KO-GFP	*Lgr5-EGFP-IRES-CreERT2;Villin-CreERT2;Mettl3*$^{fl/fl}$	TAM
Control	*Lgr5-EGFP-IRES-CreERT2*	TAM
Mettl3-Lgr5-KO	*Lgr5-EGFP-IRES-CreERT2; Mettl3*$^{fl/fl}$	TAM
Control	*Lgr5-CreERT2;Rosa26*$^{loxp\text{-}stop\text{-}loxp\text{-}ZsGreen}$	TAM
Mettl3$^{\Delta Lgr5}$	*Lgr5-CreERT2;Rosa26*$^{loxp\text{-}stop\text{-}loxp\text{-}ZsGreen}$*;Mettl3*$^{fl/fl}$	TAM

Table S2: q-PCR primer sequences, related to Figure 2, 5, 6, S1, S3 and S4.

Gene	Forward primer	Reverse primer
Gapdh	AAGAAGGTGGTGAAGCAG	TCATACCAGGAAATGAGC
Mettl3	GGTTCGTTCCACCAGTCATAA	ATCCCATCCAGTTGGTTTCC
Lgr5	CGGGACCTTGAAGATTTCCT	GATTCGGATCAGCCAGCTAC
Ascl2	GCCTGACCAAATGCCAAGTG	ATTTCCAAGTCCTGATGCTGC
Klf9	TTATTGCACGCTGGTCACTATC	CTCATCGGGACTCTCCAGAC
Fosb	CAATCACAACCAGCCAGGAT	GGCATGTCATAAGGGTCAACA
Purb	CTTCAGCAAAGAGCCCAAATAC	CCTGCCAAGTCTTGATCCTAA
Tcf3	TTGACCCTAGCCGGACATA	CACTGGTGTCTCTCCCAAAG
Vdr	ACGCCAAGATGATCCAGAAG	GGAGATCTCATTGCCGAACA
Jun	CCTTCTACGACGATGCCCTC	GGTTCAAGGTCATGCTCTGTTT
Nr3c1	AAGCTTCGGGATGCCATTAT	TCGAGCTTCCAGGTTCATTC
Egr1	AGGAGTGATGAACGCAAGAG	GGATGGGTAAGAAGAGAGTGAAG
Fos	CGGGTTTCAACGCCGACTA	TTGGCACTAGAGACGGACAGA
Olfm4	CGAGACTATCGGATTCGCTATG	TTGTAGGCAGCCAGAGGGAG
Alpi	GTCCCACCGCTGGTTACTTT	CTGTGGGCTGAGATGATGTC
Lyz	ACGAGCTACAAACTACAACCG	GATCTCTCACCACCCTCTTTG
Axin2	GCTCCAGAAGATCACAAAGAGC	AGCTTTGAGCCTTCAGCATC
C-myc	GCTGTTTGAAGGCTGGATTTC	GATGAAATAGGGCTGTACGGAG
Ki67	AGGCTCCGTACTTTCCAATTC	CGTCTTAAGGTAGGACTTGCAG
Muc2	TGTGGTCTGTGTGGGAACTTTG	GCTTACATCTGGGCAAGTGGAA
Defa	GCACAGAAGGCTCTGCTCTT	ACCCAGATTCCACATTCAGC
Spink4	TGCAGTCACATAGCTCACAAG	CCATGCCAAGGAGGGGAA
Agr2	TGTCCCCAGAATTGTGTTTGTAGA	TGTCAGAAGGTTCATAAGCGTAGA
Chga	GCTGGAACATAAGCAGGAGG	ATCCTGCTCCATCGCTTG
Gcg	CTTCCCAGAAGAAGTCGCCA	GTGACTGGCACGAGATGTTG
Reg4	CTGAGCTGGAGTGTCAGTCAT	GTCCACTGCCATAATTGCTTCT
Cbr1	TCAATGACGACACCCCCTTC	CCTCTGTGATGGTCTCGCTTC
Dclk	CAGCAAGTCTCCCAGAAGATAC	GGACTGTGTAACAGGAGTGAAA

Table S3: sgRNA sequence, related to Figure 4.

Species	**Gene**	**Target +PAM**
Mouse	***Ascl2***	GTGGACGTTTGCACCTTCACGGG
	Klf9	CTTAAAAAGTTCTCGCGCTGGG
	Fosb	GAACCAGCTACTCAACCCCAGG
	Purb	ATCTTGAGGAAGCGGCCCTTGG
Human	***METTL3***	CTTGAGTGGCAGGAGCATCTGG
	NC	GCGCGATAGCGCGAATATAC

Table S4: RRACH enriched 3'UTR sequence, related to Figure 4.

TF		Sequence (RRACH motifs were marked with red color, A/T was marked by underline)
Ascl2	3'UTR-WT	CTTCCGGACCTTGCAGCATCAGGACTTGGAAATTTCTCAGGATAAAGATTTTTACAATGACAATCTACTTTTTATCAATTAACTTGAACTGTTGTAGGACTCTACTG
	3'UTR-mut	CTTCCGGTCCTTGCAGCATCAGGTCTTGGAAATTTCTCAGGATAAAGATTTTTACAATGACAATCTACTTTTTATCAATTAACTTGATCTGTTGTAGGTCTCTACTG
Klf9	3'UTR-WT	ATCTAAAGACTTGAAAACAAAACAACAACAACAAAAAGTTACTTATAGTCAATGGATAAGCAGAGTCCGAATTTACACTAATCAAGACAGACCTTCGAGGGGTCACGATAAGTCCGGAACTTTCAAACCTTGCTTCGTATGAATTGTACTATCTGAACATAAACTGCACT
	3'UTR-mut	ATCTAAAGTCTTGAAAACAAAACAACAACAACAAAAAGTTACTTATAGTCAATGGATAAGCAGAGTCCGAATTTACACTAATCAAGACAGACCTTCGAGGGGTCACGATAAGTCCGGATCTTTCAATCCTTGCTTCGTATGAATTGTACTATCTGATCATAATCTGCACT
Fosb	3'UTR-WT	CCGCTGAACTCGCCCTCCCTTCTTGCTCTGTAAACTCTTTAGACAAACAAAACAAACAAACCCGCAAGGAACAAGGAGGAGGAAGATGAGGAGGAGAGGGGAGGAAGCAGTCCGGGGGTGTGTGTGTGGACCCTTTGA
	3'UTR-mut	CCGCTGATCTCGCCCTCCCTTCTTGCTCTGTAAACTCTTTAGACAAACAAAACAAACAAACCCGCAAGGATCAAGGAGGAGGAAGATGAGGAGGAGAGGGGAGGAAGCAGTCCGGGGGTGTGTGTGTGGTCCCTTTGA
Purb	3'UTR-WT	CCGTATGAACCAGAGAATTATGGCTAATTCGGCTGTTACAGCCACTGGCTGGCTGCATTTTAAACCTTAAAACTTGACTATCTGCAAAAAAGGAACAGTGTGGCTACAAGCCTGAGCTTTAATGAAATAGACATCCTCACAGAGAAGTTGGAAATAACAGAACTGAAGTC
	3'UTR-mut	CCGTATGATCCAGAGAATTATGGCTAATTCGGCTGTTACAGCCACTGGCTGGCTGCATTTTAAACCTTAAATCTTGACTATCTGCAAAAAAGGATCAGTGTGGCTACAAGCCTGAGCTTTAATGAAATAGTCATCCTCACAGAGAAGTTGGAAATAACAGATCTGAAGTC

Supplemental Experimental Procedures

Immunoblotting

The following antibodies were used for immunoblotting: METTL3 (1:1000, Abcam, ab195352), ASCL2 (1:500, Abclonal, A20194), KLF9 (1:1000, Novus Biologicals, NBP-04457-100µl), FOSB (Abcam, 1:1000, ab184938), PURB (1:1000, Proteintech, 18128-1-AP), TUBULIN (1:1000,MBL, PM054-7) and GAPDH (1:1000, MBL, M171-7).

ChIP-seq

After crosslink with 1% formaldehyde and stopped with glycine, organoids were re-suspended in SDS cell lysis buffer (0.3% SDS, 50mM Tris-HCl, pH 8.0, 20mM EDTA, 1X EDTA-free protease inhibitor cocktail). The crosslinked DNA was sheared to lengths between 100 bp and 2500 bp with sonication, and diluted in DB buffer (16.7mM Tris-HCl, pH 8.0, 0.01% SDS, 1.2mM EDTA, 1.1% Triton X-100, 1X EDTA-free protease inhibitor cocktail). After pre-cleared with 30 µL of 1:1 protein A/G Dyna beads (Life Technologies, 10001D/10003D), the samples were incubated with anti-FOSB antibody (Abcam, ab184938) overnight at 4 ^{o}C, then washed 5 times with 1 mL of RIPA buffer (50mM Hepes, pH 8.0, 1% NP-40, 0.7% DOC, 0.5M LiCl, 1X EDTA-free protease inhibitor cocktail) and once with 1mL TE buffer. The beads were eluted in 100 µL of Elution buffer (10 mM Tris-HCl, pH 8.0, 1% SDS, 1 mM EDTA) for 30 min at 65 ^{o}C. The Protein-DNA complexes were reversed crosslink at 65 ^{o}C overnight. After incubation at 55 ^{o}C for 1 hour to digest proteins with 0.4mg/mL Proteinase K (AMRESCO, 0706-100mg) and another 1 hour at 37 ^{o}C to digest RNA with 0.4mg/mL RNase A (Thermo Scientific, EN0531), DNA were purified by phenol chloroform and ethanol-precipitated. Purified DNA was subjected to Tru-seq library construction using NEBNext Ultra II DNA Library Prep Kit for Illumina (NEB, E7645S). The library was purified and size-selected with AMPure XP beads (Beckman, A63881) and sequenced as paired-end with Illumina Novaseq 6000. HISAT2 was used to align the sequences to the mouse genome and generate bam files. After deprived of PCR duplicates using Picard tools, Deeptools bamCoverage (CPM normalized and extended reads) was used to generate bigwig files from bam files. MACS2 was used for peak calling and to generate bed files from aligned reads. HOMER annotatePeaks.pl was used to annotate the peaks.

MeRIP-seq analysis

The cDNA libraries were generated using SMARTER Stranded Total RNA-seq kit v2 (Takara, 634411) and sequenced on an Illumina Novaseq 6000 platform. In each sample, reads were aligned to the mouse genome in Ensembl (release 95) with HISAT2. The resulting SAM files were sorted and converted to BAM files by SAMtools and deprived of PCR duplicates using Picard tools (v1.12). m6A peaks in each sample were identified using exomePeak (v2.17.0) R/Bioconductor package with default parameters, and the corresponding input sample served as control. The significantly differential m6A peaks between Mettl3-KO-GFP and control ISCs were identified by the threshold of $|log2FC| \geq 1$ and $P<0.05$. Metagene plot was created by the Bioconductor Guitar (v2.0.0) package using the control data.

scRNA-seq normalization and clustering

Data normalization was performed using Seurat “NormalizeData” and using “LogNormalize” as the normalization method (sacle.factor=100000). Variable genes were detected using “FindVariableFeatures”. We used “FindIntegrationAnchors” to combine the control library and *Mettl3*-KO-GFP library, and the scaled gene expression data were projected onto principal components (PCs). The first 30 PCs were used for non-linear dimensionality reduction using Uniform Manifold Approximation and Projection (UMAP). Clustering was performed using the “FindNeighbors” followed

by the “FindClusters” functions. Marker genes for each cluster have been identified using “FindAllMarkers” function.

Ratio of each cell type was calculated by dividing the number of a cell type to the total number of cells. Cell cycle annotation of each cell was performed using the cell cycle scoring function in Seurat, which assigns each cell a score based on the expression of 43 marker genes for the G2/M phase and 54 marker genes for the S phase.

Gene set enrichment analysis (GSEA) and Gene ontology (GO) analysis

To define ISC signature genes, proliferation and other cellular events, we curated and referred to previous studies. Specifically, we used 384 genes that were highly expressed in $Lgr5^{high}$ ISCs (Munoz et al., 2012) for stem cell signature genes, 43 marker genes for G2/M phase and 54 marker genes for S phase for proliferation genes (Tirosh et al., 2016), Notch (HALLMARKS), Wnt (Fevr et al., 2007), P53 (HALLMARKS), MAPK (Basak et al., 2017), YAP (Imajo et al., 2015), Regeneration (Wang et al., 2019), Fetal genes (Mustata et al., 2013), differentiation genes (Haber et al., 2017) and apoptosis death-related genes (HALLMARKS).

GSEA (v.4.0) (Subramanian et al., 2005) was performed on the pre-ranked gene list as described above. Differentially expressed genes were identified using DESeq2 (v1.24.0) (Love et al., 2014). Genes with $P<0.05$ and absolute value of $|\log_2FC|>1$ were used for GO analysis, which was performed using the web tool: DAVID (Dennis et al., 2003) (http://david.abcc. ncifcrf.gov/). GO terms with $P < 0.05$ were determined to be statistically significant. Radar charts were plotted using the R software package fmsb (v0.7.1).

Motif identification

HOMER (v4.10.0) (Heinz et al., 2010) was used to call the motifs enriched in m^6A peaks or transcription factor motifs. For ChIP-seq, findMotifsGenome.pl was used to call transcription factor motifs enriched at peaks. For MeRIP-seq, findMotifs.pl was used, and the motif length was restricted to 6 nucleotides. All peaks mapped to mRNAs were used as the target sequences, and background sequences were constructed by randomly shuffling peaks upon total mRNAs using BEDTools’ shuffleBed (v2.18) (Quinlan and Hall, 2010).

scRNA-seq pseudotime analysis

Pseudotime analysis with the filtered data from Seurat was performed using Dyno (Saelens et al., 2019) and Monocle 2 (Qiu et al., 2017). Dimensionality reduction and trajectory reconstruction were carried out with the advanced nonlinear reconstruction algorithm paga_tree and DDRTree to determine two components, respectively.

Supplemental references

Basak, O., Beumer, J., Wiebrands, K., Seno, H., van Oudenaarden, A., and Clevers, H. (2017). Induced Quiescence of Lgr5+ Stem Cells in Intestinal Organoids Enables Differentiation of Hormone-Producing Enteroendocrine Cells. Cell Stem Cell *20*, 177-190 e174. 10.1016/j.stem.2016.11.001.

Dennis, G., Jr., Sherman, B.T., Hosack, D.A., Yang, J., Gao, W., Lane, H.C., and Lempicki, R.A. (2003). DAVID: Database for Annotation, Visualization, and Integrated Discovery. Genome Biol *4*, P3.

Fevr, T., Robine, S., Louvard, D., and Huelsken, J. (2007). Wnt/beta-catenin is essential for intestinal homeostasis and maintenance of intestinal stem cells. Mol Cell Biol *27*, 7551-7559.

10.1128/MCB.01034-07.

Haber, A.L., Biton, M., Rogel, N., Herbst, R.H., Shekhar, K., Smillie, C., Burgin, G., Delorey, T.M., Howitt, M.R., Katz, Y., et al. (2017). A single-cell survey of the small intestinal epithelium. Nature *551*, 333-339. 10.1038/nature24489.

Heinz, S., Benner, C., Spann, N., Bertolino, E., Lin, Y.C., Laslo, P., Cheng, J.X., Murre, C., Singh, H., and Glass, C.K. (2010). Simple combinations of lineage-determining transcription factors prime cis-regulatory elements required for macrophage and B cell identities. Mol Cell *38*, 576-589. 10.1016/j.molcel.2010.05.004.

Imajo, M., Ebisuya, M., and Nishida, E. (2015). Dual role of YAP and TAZ in renewal of the intestinal epithelium. Nat Cell Biol *17*, 7-19. 10.1038/ncb3084.

Love, M.I., Huber, W., and Anders, S. (2014). Moderated estimation of fold change and dispersion for RNA-seq data with DESeq2. Genome Biol *15*, 550. 10.1186/s13059-014-0550-8.

Munoz, J., Stange, D.E., Schepers, A.G., van de Wetering, M., Koo, B.K., Itzkovitz, S., Volckmann, R., Kung, K.S., Koster, J., Radulescu, S., et al. (2012). The Lgr5 intestinal stem cell signature: robust expression of proposed quiescent '+4' cell markers. EMBO J *31*, 3079-3091. 10.1038/emboj.2012.166.

Mustata, R.C., Vasile, G., Fernandez-Vallone, V., Strollo, S., Lefort, A., Libert, F., Monteyne, D., Perez-Morga, D., Vassart, G., and Garcia, M.I. (2013). Identification of Lgr5-independent spheroid-generating progenitors of the mouse fetal intestinal epithelium. Cell Rep *5*, 421-432. 10.1016/j.celrep.2013.09.005.

Qiu, X., Mao, Q., Tang, Y., Wang, L., Chawla, R., Pliner, H.A., and Trapnell, C. (2017). Reversed graph embedding resolves complex single-cell trajectories. Nat Methods *14*, 979-982. 10.1038/nmeth.4402.

Quinlan, A.R., and Hall, I.M. (2010). BEDTools: a flexible suite of utilities for comparing genomic features. Bioinformatics *26*, 841-842. 10.1093/bioinformatics/btq033.

Saelens, W., Cannoodt, R., Todorov, H., and Saeys, Y. (2019). A comparison of single-cell trajectory inference methods. Nat Biotechnol *37*, 547-554. 10.1038/s41587-019-0071-9.

Subramanian, A., Tamayo, P., Mootha, V.K., Mukherjee, S., Ebert, B.L., Gillette, M.A., Paulovich, A., Pomeroy, S.L., Golub, T.R., Lander, E.S., et al. (2005). Gene set enrichment analysis: a knowledge-based approach for interpreting genome-wide expression profiles. Proc Natl Acad Sci U S A *102*, 15545-15550. 10.1073/pnas.0506580102.

Tirosh, I., Izar, B., Prakadan, S.M., Wadsworth, M.H., 2nd, Treacy, D., Trombetta, J.J., Rotem, A., Rodman, C., Lian, C., Murphy, G., et al. (2016). Dissecting the multicellular ecosystem of metastatic melanoma by single-cell RNA-seq. Science *352*, 189-196. 10.1126/science.aad0501.

Wang, Y., Chiang, I.L., Ohara, T.E., Fujii, S., Cheng, J., Muegge, B.D., Ver Heul, A., Han, N.D., Lu, Q., Xiong, S., et al. (2019). Long-Term Culture Captures Injury-Repair Cycles of Colonic Stem Cells. Cell *179*, 1144-1159 e1115. 10.1016/j.cell.2019.10.015.